FULL PAPER

Dynamic Fluoroalkyl Polyethylene Glycol Co-Polymers: A New Strategy for Reducing Protein Adhesion in Lab-on-a-Chip Devices

*Mahesh K. Sarvothaman, Kris S. Kim, Brendon Seale, Peter M. Brodersen, Gilbert C. Walker, and Aaron R. Wheeler**

Non-specific adsorption of biomolecules (or "biofouling") is a major problem in microfluidics and many other applications. The problem is particularly pernicious in digital microfluidics (DMF, a technique in which droplets are manipulated electrodynamically on an array of electrodes coated with a hydrophobic insulator), as local increases in surface energy that arise from fouling can cause droplet movement to fail. We report a new solution to this problem: a device coating bearing a combination of fluorinated poly(ethylene glycol) functionalities (FPEG) and perfluorinated methacrylate (FA) moieties. A range of different FPEG-FA copolymers were synthesized containing varying amounts of FPEG relative to the fluorinated backbone. Coatings with low%FPEG were found to result in significant reductions in protein adsorption and improvements in device lifetime (up to 5.5-fold) relative to the state of the art. An analysis of surface topology and chemistry suggests that FPEG-FA surfaces undergo a dynamic reconstruction upon activation by applying DMF driving potentials, with FPEG groups forming vertical protrusions out of the plane of the device surface. An analysis of changes in surface wettability and adhesion as a function of activation supports this hypothesis. This innovation represents an advance for digital microfluidics, and may also find use in other applications that are currently limited by biofouling.

1. Introduction

For the past two decades, chemists have been integral players in the development of so-called "labs-on-a-chip," motivated by advantages such as rapid reagent delivery and heat transfer, precise control over short-lived intermediates, and reduced reagent use and waste generation.[1–6] Many lab-on-a-chip methods are implemented in enclosed micrometer-dimension channels (or "microchannels"), but an alternative paradigm, known as "digital microfluidics" is growing in popularity. In digital microfluidics (DMF), discrete volumes of liquids are manipulated electrostatically by the application of a sequence of potentials to an array of electrodes coated with a hydrophobic insulator.[7] Each droplet on the array is independently controlled, and can be made to mix and merge with any other droplet, offering unparalleled process control for chemical reactions. These advantages have been leveraged in applications ranging from multiplexed chemical synthesis[8–12] to integrated cell culture and analysis.[13–18]

A challenge for all lab-on-a-chip techniques is the non-specific adsorption of biomolecules to device surfaces (or "biofouling"). The large surface area-to-volume ratio of both types of microfluidic systems (microchannels and DMF) results in enhanced biofouling, which leads to sample loss and cross-contamination. A popular strategy to combat this problem is to coat device surfaces with hydrophilic/non-charged materials that swell with water and resist non-specific adsorption. This strategy has been used repeatedly in microchannels, with many reports of hydrophillic/non-charged surface coatings including polyethylene glycol (PEG)[19,20] and other materials.[21,22] Unfortunately, this strategy is not tenable for digital microfluidics, as DMF devices must have low surface energy (i.e., be hydrophobic) to reduce friction, which enables aqueous droplet translation. Thus, most DMF device surfaces are formed from fluoropolymers such as Teflon-AF (DuPont) or Cytop (Asahi Glass), which have low surface energy, but are (unfortunately) susceptible to biofouling.

Given the limits on device surface properties, previous attempts to reduce biofouling in DMF have been non-constitutive (i.e., have not involved modification of the device structure itself). Examples include immersion of droplets in a water-immiscible oil,[23,24] biasing the driving potential to favor adsorption/repelling of particular analytes,[25] stripping

Dr. M. K. Sarvothaman, K. S. Kim, B. Seale, Dr. G. C. Walker, Dr. A. R. Wheeler
Department of Chemistry
University of Toronto
80 St George St., Toronto, ON M5S 3H6, Canada
E-mail: aaron.wheeler@utoronto.ca
Dr. A. R. Wheeler
Institute of Biomaterials and Biomedical Engineering
University of Toronto
164 College St., Toronto, ON M5S 3G9, Canada
Dr. M. K. Sarvothaman, Dr. A. R. Wheeler
Donnelly Centre for Cellular and Biomolecular Research
160 College St., Toronto, ON M5S 3E1, Canada
Dr. P. M. Brodersen
Surface Interface Ontario
University of Toronto
200 College St., Toronto, ON M5S 3E5, Canada

DOI: 10.1002/adfm.201402218

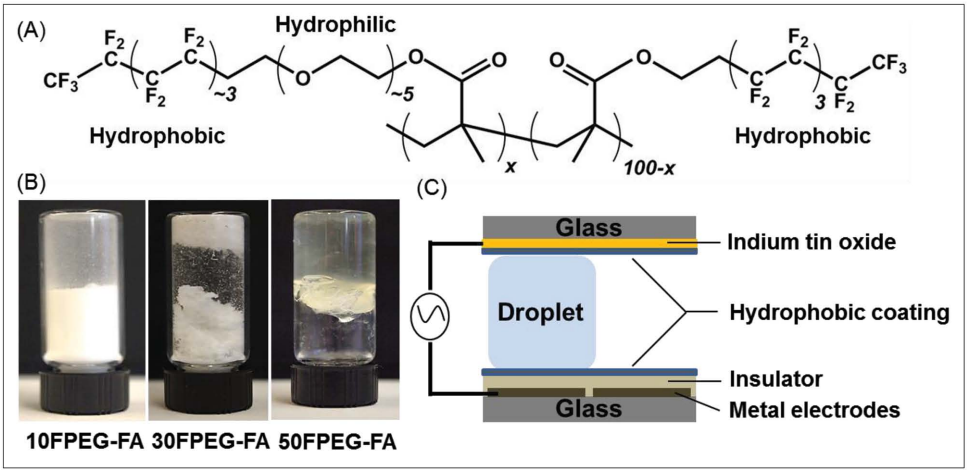

Figure 1. FluoroPEG-co-fluoromethacrylate (FPEG-FA): a new class of device coatings for digital microfluidics. A) Structure of x(FPEG-FA), where x ≈ 0.5, 1, 2, 5, 10, 30 and 50 mol% FPEG units. B) Pictures of 10FPEG-FA (coarse powder), 30FPEG-FA (fibril-like), and 50FPEG-FA (resembles an elastomer) showing the effect of FPEG composition on bulk properties. C) Side-view schematic of a DMF device showing a droplet sandwiched between the hydrophobic surfaces of the two plates.

and re-application of coverings between experiments,[26] and solution-additives to reduce fouling.[27–29] These strategies are useful and are appropriate for specific applications, but they are not universal. A universal strategy would comprise a modification to the device itself, which could then be used for any application. We introduce such a strategy here.

We report the synthesis, application, and characterization of a new polymer coating, and describe its application to digital microfluidics. As shown in **Figure 1**, the new coating is an amphiphilic copolymer of fluorinated polyethylene glycol (FPEG) residues and perfluorinated methacrylate (FA) moieties. This new "FPEG-FA" copolymer coating was inspired by the marine antifouling literature,[30–33] and results in significant reductions in biofouling in digital microfluidics. Most interestingly, the act of DMF droplet operation is observed to cause the FPEG-FA material to become "activated." Evaluation of this effect by fluorescence microscopy, atomic force microscopy, X-ray photoelectron spectroscopy, and contact angle measurements suggests that the material undergoes a rapid voltage-mediated rearrangement at the air-(or liquid)-polymer interface. This phenomenon, which has not been reported before, may be worth exploring for application to the wide range of applications that could benefit from the ability to dynamically generate patterns with varying surface properties.

2. Results and Discussion

2.1. Device Coatings

DMF devices must have surfaces with high hydrophobicity (i.e., aqueous contact angles ~110–120°) to be capable of manipulating aqueous droplets. In practice, this is typically accomplished by coating DMF devices with amorphous fluoropolymers such as Teflon-AF. A major shortcoming of such surfaces is their vulnerability to biofouling, which can be exacerbated for DMF, as exposure to electric fields can "activate" such surfaces, increasing their tendency to foul.[34–36] With this in mind, we hypothesized that we might be able to improve upon the performance of conventional DMF device coatings by developing new materials with varying surface chemistry and hydrophob/philicity, modulus and elasticity properties, a strategy that has been useful in the development of antifouling surfaces used in marine systems.[37–39]

Here, we introduce a new type of coating for DMF devices that presents both hydrophobic and hydrophilic functionalities as surface domains.[40,41] The new copolymers were prepared by a free-radical polymerization of a perfluorinated methacrylate (FA) with PEGylated–fluoroalkyl methacrylate monomer (FPEG) using AMBN as an initiator. The macromolecular architecture of the resultant copolymers has a random distribution of two co-monomer graft-chains of FA and FPEG appended to a fluorocarbon backbone (Figure 1A). The feed composition was varied to obtain a series of copolymers with different content of PEGylated-fluoroalkyl co-units. We labeled the copolymers according to the molar composition of the FPEG co-units in the copolymer; e.g., "50FPEG-FA" has ≈50 mol% of FPEG in the copolymer (Table S1 in the Supporting Information). In designing the material, we anticipated that the perfluoroalkyl grafts would impart maximum hydrophobicity for moving droplets while the grafted FPEG units would allow for resistance of protein adsorption.

The combination of rigid fluoropolymer chains with flexible FPEG-units resulted in a series of copolymers with widely varying bulk properties. For example, 50FPEG-FA resembles a transparent elastomer like polydimethyl siloxane (PDMS), 30FPEG-FA is soft and fibril-like, and 10FPEG-FA is a coarse powder (Figure 1B). It follows that the addition of FPEG-chains to the copolymer increases the elasticity and lubricity, and we hypothesized that this would improve the resistance to biofouling (and thus result in improved device performance) for digital microfluidics.

In typical DMF applications, droplets are manipulated in a "two-plate" format, sandwiched between two coated substrates (Figure 1C). Initial experiments with manipulation of water droplets led to an important observation: devices that are coated

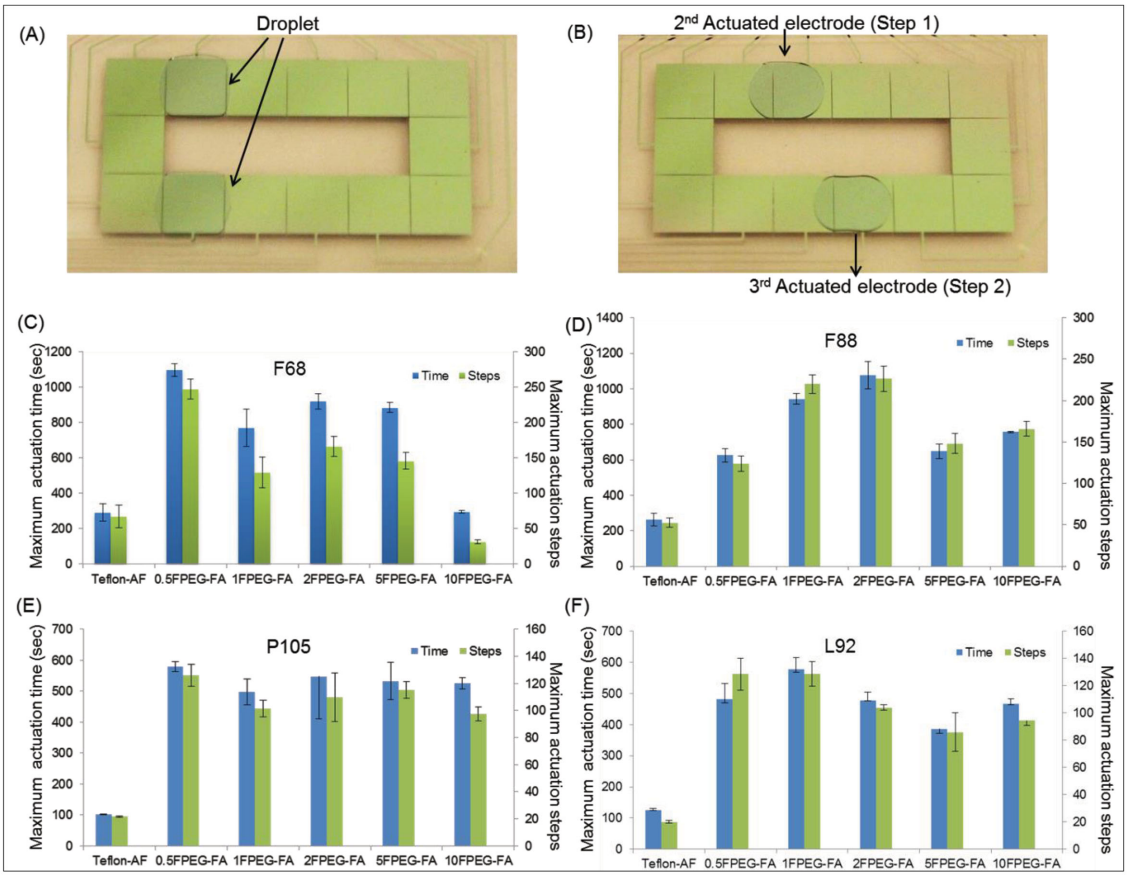

Figure 2. Device longevity assay. A,B) show frames from a movie depicting the movement of two droplets on device one during a longevity assay. In (A), two droplets are shown in an initial position. In (B), the droplet at the top of the device has completed one step, and the droplet at the bottom of the device has completed two steps. In each assay, a droplet was actuated back and forth across four electrodes until droplet movement failure was observed. C–E) Maximum actuation time (blue bars, left axes) and the maximum number of steps (green bars, right axes) for DMF device bottom plates coated with Teflon-AF and 0.5, 1, 2, 5, and 10FPEG-FA. Droplets contained cell culture medium supplemented with 10% serum and one of four Pluronic additives: A) F68, B) F88, C) P105, D) L92. Each condition was repeated three times on two different devices, and error bars represent ± 1 S.D.

with FPEG-FA containing relatively low FPEG content (i.e., 10% or less) support droplet movement with similar characteristics (velocity, reliability, etc.) to those coated with Teflon-AF. In contrast, in devices that are coated with FPEG-FA with high FPEG content (i.e., 30% and 50%) droplets move very slowly or not at all. This is consistent with our expectation – too many FPEG groups on the surface likely increases the surface energy such that aqueous droplets experience high friction, reducing the ability for droplets to move. After ascertaining that the new coatings (those with low FPEG content) support aqueous droplet movement, we were ready to evaluate their hypothesized resistance to biofouling.

2.2. Device Longevity

When digital microfluidic devices are used to manipulate aqueous droplets containing proteins and other biomolecules for extended periods of time, non-specific adsorption increases the surface energy and eventually renders the device inoperable. Thus, a quantitative assay for device lifetime[27] was used to evaluate the performance of the new FPEG-FA coatings. As shown in **Figure 2**A–B, droplets were driven back and forth along a path of four electrodes until the droplets were no longer moveable, recording the time and the number of electrode steps.

Cell culture media containing 10% serum, a concentrated mixture of proteins, amino acids, salts, sugars, and other constituents, was used as a "worst case" test matrix for these experiments. This mixture is so problematic for DMF that it has a device lifetime of "zero" under standard conditions; that is, for this mixture, surface fouling is immediate, and droplets are completely unmovable. To facilitate droplet movement, the mixture was supplemented with pluronic (block copolymers of polyethylene oxide, PEO and polypropylene oxide, PPO) additives, a common strategy for increasing DMF device lifetime.[27,28] Four pluronic species, F68, F88, P105 and L92, were chosen to span a broad range of molecular weights and PEO/PPO ratios and block lengths.

The results of the device longevity assay are shown in Figure 2C–F, which leads us to several conclusions. First and most importantly, FPEG-FA-coated devices are superior to standard Teflon-AF-coated devices regardless of which pluronic additive is used. These improvements are significant; for

example, using a 0.5FPEG-FA coating instead of a Teflon-AF coating for P105-containing droplets extends the device lifetime from 102 to 580 actuation steps (representing a 5.5-fold increase in the number of steps). This extension should dramatically improve the ability of DMF devices to perform long-term, multi-day assays, as the DMF cell culture and analysis experiments reported previously[13–16] have used a few (≈20–40) droplet actuation steps per day punctuated by long periods of incubation.

Second, in general terms, coatings with lower%FPEG perform better — i.e., for most conditions tested, devices coated with 0.5FPEG-FA, 1FPEG-FA, 2FPEG-FA, and 5PEG-FA had longer lifetimes than devices coated with 10FPEG-FA. Third, there are subtle differences in device performance when used with different pluronic additives — for example, F68 and F88 have similar ratios of PPO/PEO but different molecular weights (F68: 8400 Da, F88: 11,400 Da), and the best coating for droplets containing F68 is 0.5FPEG-FA, while the best coating for droplets containing F88 is 2FPEG-FA. Thus, we recommend that future users may want to consider which additives are to be used when choosing the FPEG% of the coating.

To validate the effects on device longevity, a second test was run using an automated DMF actuation system.[42] A program was developed to continuously manipulate droplets of cell culture media containing P105 on devices coated with 1FPEG-FA or with Teflon-AF until capacitance measurements failed to meet a set threshold. As shown in Figure S1, Supporting Information, the FPEG-coated devices had approximately 3× greater longevity when compared to Teflon-AF-coated devices. Further, the instantaneous velocities logged for droplets on the Teflon-AF-coated devices were observed to decrease gradually as a function of time (consistent with biofouling-mediated failure), while those for FPEG-coated devices were observed to remain constant (suggesting that the failure mechanism was not biofouling).

To confirm that the device lifetime observations correlate with protein fouling, a series of experiments were conducted using FITC-labeled bovine serum albumin (FITC-BSA) as a tracer.[28] DMF device surfaces were exposed to the tracer under both passive conditions (incubation with tracer for 1 or 10 h with no electric field) and active conditions (incubation with tracer for 1 or 5 min while applying DMF driving potential). The results (Figure S2, Supporting Information) show that Teflon-AF-coated devices have the highest level of fouling, and among the FPEG-FA coated devices, the lowest fouling levels are observed for the low%FPEG surfaces (i.e., 0.5FPEG-FA, 1FPEG-FA, 2FPEG-FA, and 5FPEG-FA). Moreover, the low%FPEG surfaces are the most stable over time – for these surfaces, there was little change between 1 and 10 h of passive fouling or 1 and 5 min of active fouling. These results are consistent with protein fouling being the cause of device failure and resistance to this effect being the source of improvement in device lifetime in Figure 2.

The near-perfect superiority of the FPEG-FA coatings relative to Teflon-AF for device longevity (i.e., 19 out of 20 conditions tested in Figure 2C–F) suggests several interesting questions. What is the mechanism of the observed effects? Further, are the FPEG-FA coatings simply better at resisting biofouling on "passive" surfaces? Or are FPEG-FA coatings particularly well suited for resisting fouling after application of driving voltages? Experiments designed to probe these questions are described below.

2.3. Surface Topography and Dynamics

Surface topography plays an important role in the wetting behavior of polymer coatings,[43,44] and we hypothesized that the topography of FPEG-FA surfaces might be related to the device longevity effects described above. To test this hypothesis, atomic force microscopy (AFM) was used to evaluate "passive" (i.e., native devices, never used) and "activated" (i.e., devices that had been exposed to a potentiated droplet and then dried) surfaces coated with 1, 5, and 30FPEG-FA, as well as Teflon AF. As shown in **Figure 3**A, all of the passive surfaces were smooth, with root-mean square (RMS) roughness values ranging from 0.2–0.9 nm. By contrast, the activated surfaces were markedly roughened, with RMS roughness values of 7.0, 10, 1.4, and 4.5 nm for 1, 5, and 30FPEG-FA and Teflon-AF, respectively. Interestingly, the ≈nm scale of these roughened features are similar to the dimensions of proteins in solution. Moreover, the coatings that show the greatest changes in surface roughness, 1 and 5FPEG-FA, are those that correspond to the highest device lifetimes (Figure 2). As far as we are aware, this is the first observation or report that digital microfluidic droplet actuation affects the topography of a device surface.

AFM phase images of the surfaces (Figure 3B–D) reveal additional observations about the nature of the topographical dynamics. The phase distribution for Teflon-AF is nearly the same for the passive and activated surfaces, while the phase distributions for FPEG-FA surfaces vary considerably upon activation, with notable differences associated with FPEG content. For the FPEG-FA surfaces, we hypothesize that the phase changes upon activation represent the migration of FPEG domains relative to the fluoroalkyl bulk material. These domains appear scattered for low FPEG-content coatings (5FPEG), but they appear aggregated for high FPEG-content coatings (30FPEG). When viewed in the context of the roughness data (Figure 3A), the phase images are consistent with the formation of perpendicular FPEG-domain protrusions for low FPEG-content materials upon activation, while the FPEG domains seem to aggregate in the plane of the surface for high FPEG-content materials. To probe the lifetime of this effect, 5FPEG-FA surfaces were evaluated 1 h after activation and again at 30 h after activation. As shown in Figure S3 in the Supporting Information, the phase aggregation seems to disperse with time, consistent with a slow recovery to a passive-like state.

X-ray photoelectron spectroscopy (XPS) was used to probe the relationship of surface rearrangement upon exposure to DMF droplet actuation to chemical functional group composition. Carbon 1s photoelectron intensities were measured for passive and activated surfaces. As shown in **Figure 4**A, passive Teflon-AF surfaces feature peaks corresponding to -CF_3 (≈295 eV) and -CF_2- (≈292 eV). Upon activation, Teflon-AF surfaces expose a peak corresponding to -$\underline{C}$-$(CF_3)_2$ (≈285 eV), an effect previously seen for this material upon annealing.[45] As shown in Figure 4B-C, FPEG-FA surfaces also have peaks corresponding to -CF_3 and -CF_2-, but in addition have a peak corresponding to -O-C = O (≈289 eV) and overlapping contributions from -CH_2-, -CH_2-O-, and -$\underline{C}H_2$-CF_2- (≈285 eV). Figure 4D shows a quantification of peak areas corresponding to the relevant moieties. As shown, 5FPEG-FA surfaces undergo significant changes upon activation: signals originating

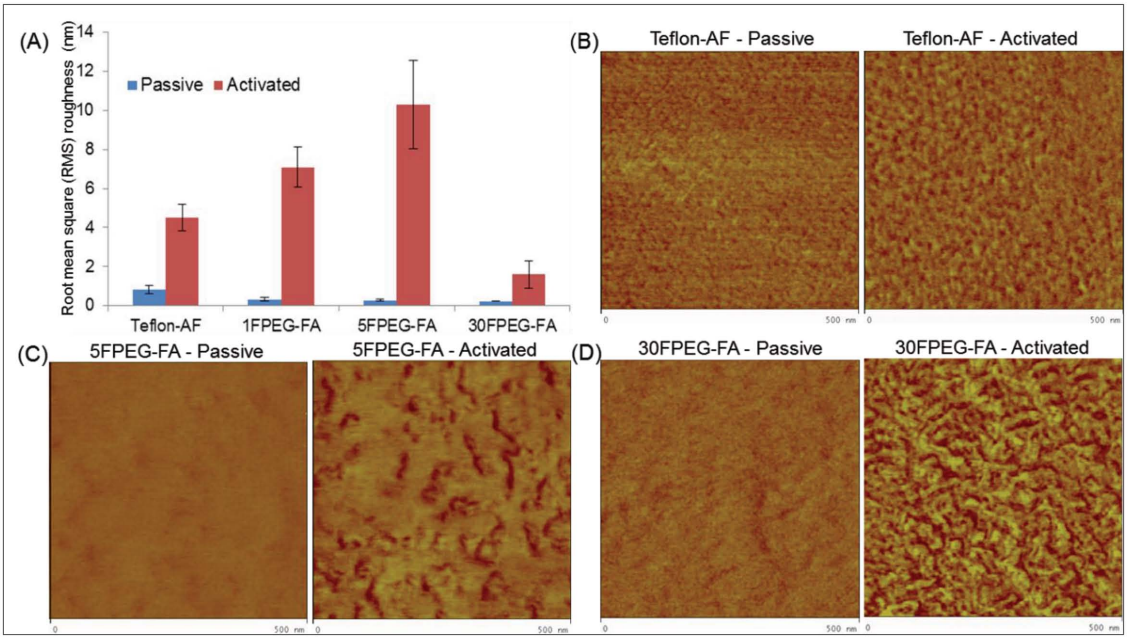

Figure 3. Surface topography and dynamics. A) Root-mean-square (RMS) roughness values determined from 2×2 μm^2 regions on AFM height images of DMF devices coated with Teflon-AF or 1, 5, or 30FPEG-FA, in passive (blue) and activated (red) state. Images were captured from three separate regions on three different devices for each condition. Error bars represent ± 1 S.D. AFM phase images (500 × 500 nm) of B) Teflon-AF, C) 5, and D) 30 FPEG-FA in passive (left) and activated (right) state.

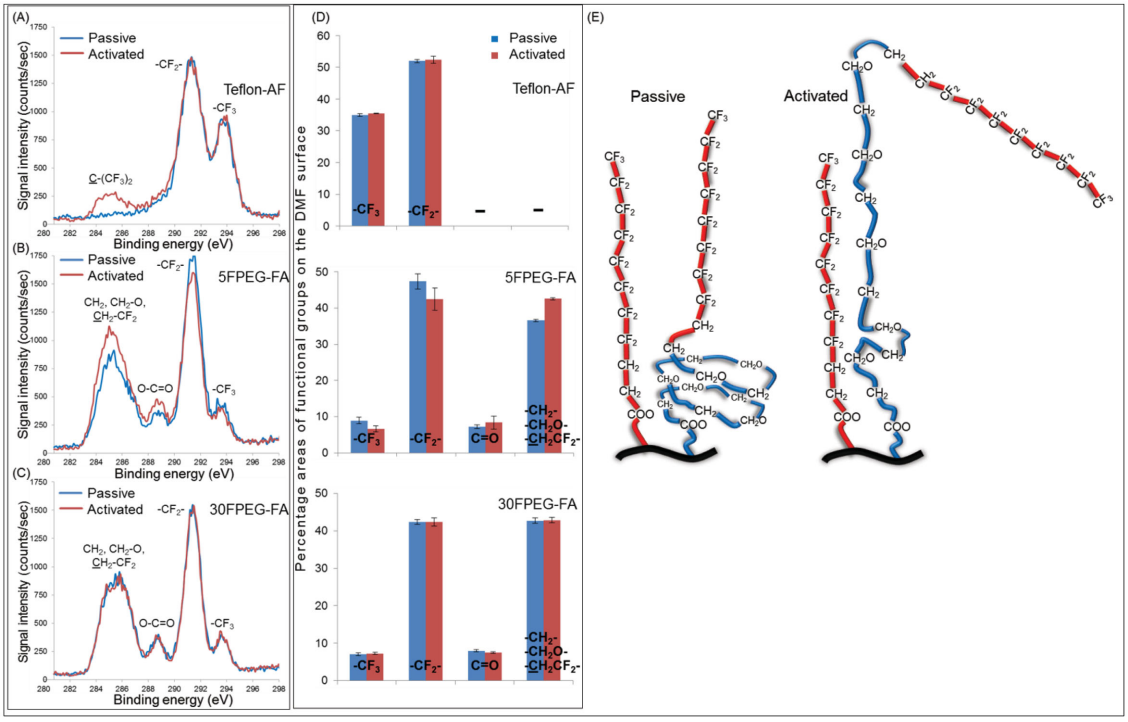

Figure 4. Surface chemistry. C-1s XPS spectra of DMF devices coated with A) Teflon-AF, B) 5FPEG-FA, and C) 30FPEG-FA in passive (blue) and activated (red) state. Peaks corresponding to -CF_3 (≈295 eV), -CF_2- (≈292 eV), -C-$(CF_3)_2$ (≈285 eV), -O-C=O (≈289 eV) and -CH_2/-CH_2-O/-CH_2-CF_2 (≈285 eV) are highlighted. D) Plot of peak areas for passive (blue) and activated (red) Teflon-AF (top), 5FPEG-FA (middle), and 30FPEG-FA (bottom). Each condition was repeated three times on two different devices, and error bars represent ± 1 S.D. E) Schematic depicting the proposed model for the dynamic behavior of the 5FPEG-FA surface from passive (left) to activated (right) upon voltage actuation.

from fluorinated moieties (-CF_3 and -CF_2-) decrease (by 2.3% and 4.8%, respectively), while signals originating from (and adjacent to) PEG (-O-C = O, -CH_2-, -CH_2-O-, and -$\underline{C}H_2$-CF_2-) increase by 6.0%. In contrast, there is little or no change observed upon activation for fluorinated or PEG groups in 30FPEG-FA.

The AFM (Figure 3) and XPS (Figure 4A–D) data together paint an interesting picture for the topographical dynamics for surfaces coated with low FPEG-content FPEG-FA. The data suggest that when a DMF driving potential is applied to an aqueous droplet positioned on such a surface, FPEG domains move from underneath the fluoroalkyl bulk to being exposed, forming perpendicular protrusions out of the plane of the device in as little as one minute of activation. This transition is represented schematically in Figure 4E.

If the mechanism proposed in Figure 4E is correct, FPEG-FA joins a few reports of materials that can be dynamically modulated by application of electric potential; however, we propose that the phenomenon reported here is uniquely well suited for DMF. For example, Lahann et al.[46] reported a surface coating in which charged moieties can be exposed or hidden depending on the polarity of an applied potential. Likewise, Yeo et al.[47] reported methods to electrochemically modify a surface to either cleave or promote attachment of a peptide that promotes cell adhesion. These methods, while exciting, require that the surface alternate between being hydrophobic and hydrophilic – completely unsuitable for DMF, which requires a hydrophobic surface (at all times) to enable aqueous droplet movement. In an alternative strategy, Shivapooja et al.[48] reported a technique to electromechanically distort a polymer surface to promote macroscale detachment effects (e.g., release of a barnacle); this strategy would also likely be untenable for DMF, as macro-scale topographical features are known to impede droplet movement.[49] Beyond DMF, materials with dynamic surface properties (such as FPEG-FA and the examples above[44–46]) are of great interest because of the potential to dynamically generate patterns with different properties for sensing and tissue engineering. But unlike the examples above,[44–46] FPEG-FA is a bulk material that can be tuned to have different mechanical properties (Figure 1B), such that it might serve as a device structure (rather than being useful only as a coating). Thus, we propose that FPEG-FA may be appropriate for applications such as drug delivery,[50] bioanalysis,[51] and therapeutics.[52]

Regardless of context, the putative mechanism represented in Figure 4E is interesting and merits study, as it is the first report of a constitutive method for DMF that can a) reduce protein adhesion (Figure S2, Supporting Information) and b) improve device longevity (Figure 2 and Figure S1, Supporting Information). To further probe this effect, we evaluated two additional properties: surface wettability and elastic modulus/adhesion.

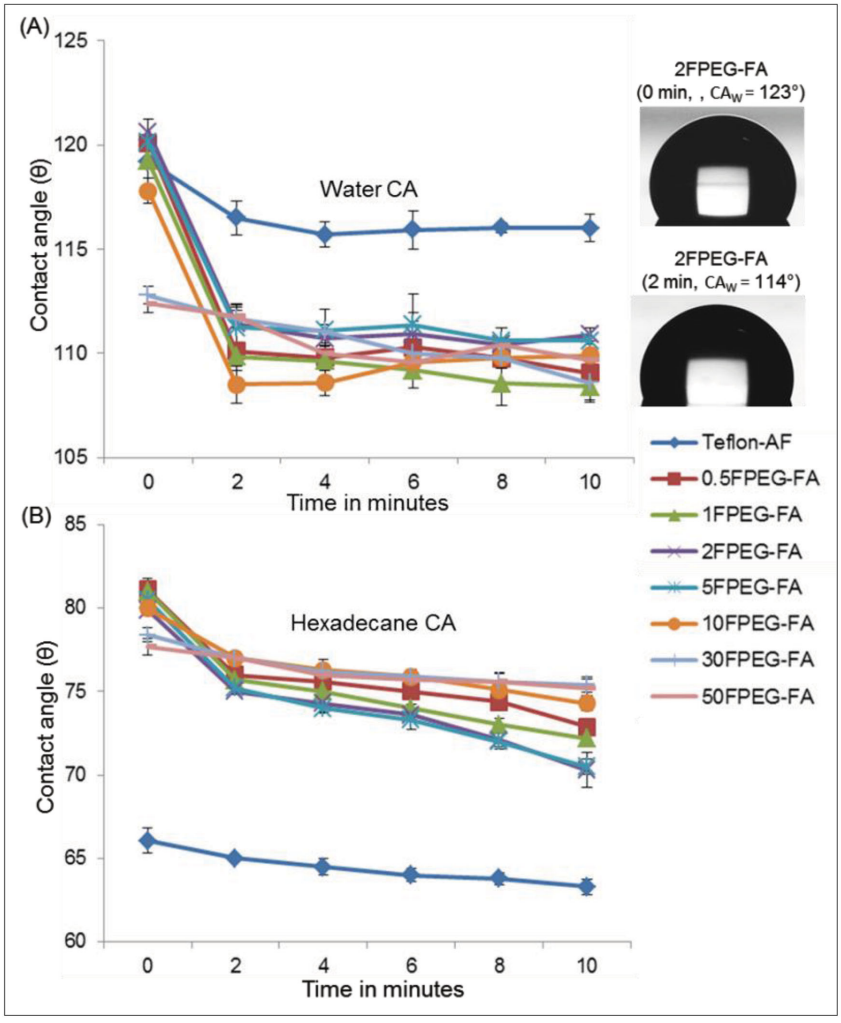

Figure 5. Surface wettability. Static contact angles measured for A) water (CA_W) and B) n-Hexadecane (CA_H) for devices after exposure to DMF driving potentials for 0, 2, 4, 6, 8, or 10 min. Devices were coated with Teflon-AF (blue diamonds), 0.5FPEG-FA (red squares), 1FPEG-FA (green triangles), 2FPEG-FA (purple Xs), 5FPEG-FA (blue asterisks), 10FPEG-FA (orange circles), 30FPEG-FA (blue lines), and 50FPEG-FA (pink without markers). Each condition was repeated six times on three different devices, and error bars represent ± 1 S.D. The images (inset) depict the change in CA_w for 2FPEG-FA upon activation for 2 min.

2.4. Surface Wettability

If the scheme depicted in Figure 4E is correct, we would expect to observe significant changes in surface wettability upon activation. That is, for low%FPEG surfaces, the contact angle for water (CA_W) should decrease as hydrophilic FPEG moieties migrate to the surface. Likewise, the contact angle for n-hexadecane (CA_H) might change, depending on the oleophobicity of FPEG relative to the fluoroalkyl bulk.

CA_W measurements were collected for surfaces after activation (by applying DMF driving potential) for 0, 2, 4, 6, 8, and 10 min. As shown in **Figure 5**A, passive FPEG-FA surfaces

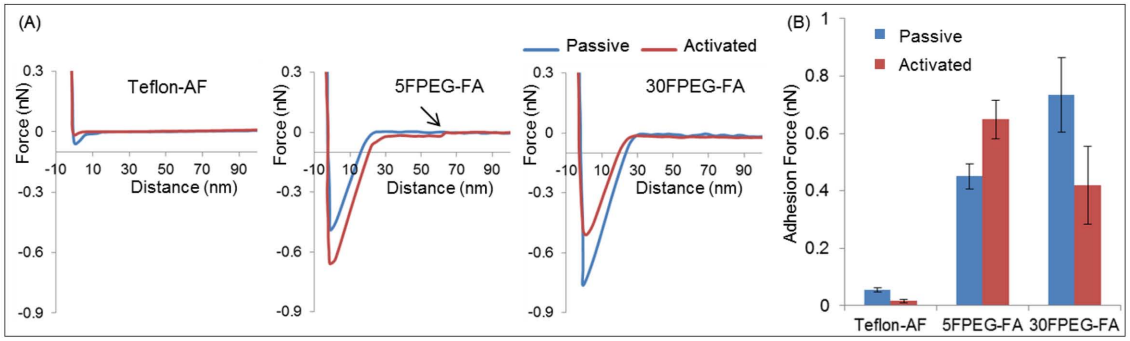

Figure 6. Surface adhesion. (A) Force – distance curves showing interaction of the AFM tip with passive (blue) and activated (red) DMF device surfaces coated with Teflon-AF (left), or 5 (middle) or 30 (right) FPEG-FA. The sharp increase in force in activated 5FPEG-FA as the tip moves away from the surface (arrow) represents regions of elastic stretching. (B) Plot of adhesion forces for passive (blue) and activated (red) surfaces. For each condition, curves were generated from three different devices at three separate regions. Error bars represent ± 1 S.D.

are hydrophobic, with CA_W measurements (after "0 min" of exposure to DMF driving potential) ranging from 114 ± 0.8° to 123 ± 1°, similar to that Teflon-AF (121 ± 0.7°). But after activation, there is a precipitous drop in CA_W, which saturates within 2–4 min. All of the surfaces exhibit this phenomenon, but the magnitude is greatest for the FPEG-FA coatings with low%FPEG content (with much as 15° reduction in CA_W within 2 min), supporting the mechanism proposed in Figure 4E. Note that these are not "active" measurements of droplet CA_W during the application of an electric field (as is often reported for electrowetting[53,54]), but rather are CA_W measurements of non-potentiated water droplets after the application and removal of an electric field (and after drying and dispensing a fresh water droplet for analysis). Thus, these measurements reflect semi-permanent changes to the material itself (e.g., surface rearrangement to expose FPEG groups) rather than temporary electrowetting-driven changes related to charge accumulation at the liquid-solid interface.

The tendency for amphiphilic polymer coatings to become "activated" under certain conditions is a well-known phenomenon; for example, many amphiphilic coatings become more hydrophilic after prolonged submersion in water.[55–57] To test this effect for the DMF devices used here, devices were submersed in water and periodically removed, dried, and probed for CA_W (Figure S4A in the supplementary materials). As expected, low%FPEG coatings become more hydrophilic within 72 h, with reductions in CA_W of similar magnitude to those observed for electric fields (Figure 5A). As far as we are aware, the data in Figure 5A are the first to show this type of effect for voltage-mediated activation of a bulk material.

To test for changes in oleophobicity, contact angle measurements for hexadecane (CA_H) were collected before and after activation by applying DMF driving potential (Figure 5B) or submersion in water (Figure S4B in the supplementary materials). Interestingly, all of the FPEG-FA coatings have CA_H values (in the range of 80° for passive surfaces) that are much higher than those for Teflon-AF (66°), suggesting that FPEG-FA is more oleophobic than Teflon-AF. Upon activation, a similar trend is observed for CA_H as is observed for CA_W, with reductions in contact angle (indicating increasing oleophilicity) for all surfaces, but with the largest changes observed for low%FPEG FPEG-FA coatings. Again, these results are consistent with rearrangement of low%FPEG FPEG-FA coatings to expose FPEG chains to the surface.

2.5. Elastic Modulus and Adhesion

As indicated by the images in Figure 1B, the surfaces evaluated in this study have widely varying elastic properties. To quantify this parameter, AFM measurements were used to generate relative Young's modulus (E) values, which ranged from stiff (Teflon-AF E = 249 kPa) to moderate (5FPEG-FA E = 152 kPa), to elastomeric (30FPEG-FA E = 32 kPa). But Young's modulus is only part of the story – if the scheme depicted in Figure 4E is correct, we would expect to observe changes in the interfacial tension between the AFM tip and the surface (particularly for low%FPEG surfaces like 5FPEG-FA) upon activation with DMF driving potential.

AFM force-distance curves were generated for Teflon-AF, 5FPEG-FA and 30 FPEG-FA (**Figure 6**A). As expected, the AFM tip experiences little adhesion when brought into contact with the stiff Teflon-AF surface (whether passive or activated). In contrast, the AFM tip experiences significant adhesion when brought into contact with passive FPEG-FA surfaces, particularly for the very soft 30 FPEG-FA. The most interesting observation is in the difference between passive and activated FPEG-FA surfaces: upon activation, the adhesion strength *increases* for 5FPEG-FA, while it decreases for 30FPEG-FA. These magnitudes of these differences (Figure 6B) are significant, and support the hypothesis outlined in Figure 4E – that is, upon activation, 5FPEG-FA surfaces rearrange to expose FPEG groups, which are attractive to the AFM tip. In addition, the sudden rise in force value after retraction in the force curve for activated 5FPEG-FA (arrow in Figure 6A, not observed for Teflon-AF or 30FPEG-FA), suggests regions of entropic stretching,[58,59] which further supports the hypothesis of significant surface rearrangement upon activation.

3. Conclusion

In an attempt to reduce the effects of biofouling in microfluidics, we designed, synthesized, and characterized amphiphilic copolymers of fluorinated polyethylene glycol (FPEG) and

perfluorinated methacrylate (FA), known as FPEG-FA. The new coatings have a significant impact on device lifetime (which is limited by biofouling), allowing for up to 5.5-fold improvement relative to the state of the art. The mechanism of these effects was examined by fluorescence microscopy, atomic force microscopy, X-ray photoelectron spectroscopy, and surface contact angle measurements. Interestingly, the enhanced lifetime (and reduced fouling) of the FPEG-FA copolymer correlates with an apparent surface reconstruction to yield physicochemical heterogeneities at the air-polymer interface. Further, this surface rearrangement appears to be driven by application of digital microfluidic driving potentials. We propose that FPEG-FA is a useful new material for digital microfluidics, and more generally, the voltage-mediated dynamic nature of this material merits consideration for applications in drug delivery, bioanalysis, and therapeutics.

4. Experimental Section

Reagents: All reagents were purchased from Sigma-Aldrich (Oakville. ON) unless specified otherwise. Methacryloyl chloride, triethylamine and dichloromethane were freshly distilled before use. Trifluorotoluene (TFT) was stored under nitrogen in a sealed bottle. The PEGylated–fluoroalkyl alcohol, Zonyl FSO-100, $F(CF_2CF_2)_4(CH_2CH_2O)_5CH_2CH_2OH$ (M_n = 700 g/mol, M_w/M_n = 1.2) was stored under vacuum overnight prior to use. 2,2′-Azodi (2-methylbutyronitrile (AMBN) (from Akzo Nobel, Concord, ON) was recrystallized from methanol and stored at 4 °C before use. 1*H*,1*H*,2*H*,2*H*-Perfluorodecyl methacrylate (FA) was used without further purification. PEGylated–fluoroalkyl methacrylate monomer (FPEG) was synthesized from Zonyl-FSO-100 and methacryloyl chloride according to a conventional esterification reaction with triethylamine as an acid-acceptor and hydroquinone as a radical inhibitor (85% yield). Parylene-C dimer was from Specialty Coating Systems (Indianapolis, IN), and Teflon-AF 1600 was from DuPont (Wilmington, DE). Deionized (DI) water had ρ = 18 MΩ cm at 25 °C.

Preparation and Characterization of FPEG-FA Copolymers: In a typical preparation of the copolymer, the co-monomers FPEG (3.23 g, 4.3 mmol) and FA (2.29 g, 4.3 mmol) were kept in a Schlenk flask under vacuum for 8–10 h. TFT (25 ml) and AMBN (82 mg) was added to this monomer mixture. The resultant solution was purged with dry nitrogen for 10 min, and then degassed by four freeze–pump–thaw cycles. The flask was sealed and the mixture was stirred at 65 °C for 65 h. The copolymer was precipitated in methanol (300 mL) and kept under vigorous stirring for 10 h. It was then allowed to settle, separated from the supernatant solution, and purified by repeated precipitations from chloroform solutions into methanol (yield 70%). The copolymer described above contained 50 mol% FPEG co-units; other variations were formed containing 0.5, 1, 2, 5, 10, 30% FPEG co-units with percentages determined by NMR (as described in the Supporting Information).

DMF Device Fabrication, Assembly, and Operation: Digital microfluidic devices were fabricated in the University of Toronto Nanofabrication Center (TNFC). Patterned chromium electrodes on glass, used as bottom plates of DMF devices, were formed by photolithography and etching as described previously.[60] Three device designs were used; device one featured an array of fourteen square (4 × 4 mm) actuation electrodes, device two featured an array of eight rectangular (16.4 × 6.7 mm) electrodes, and device three featured an array of 80 square actuation electrodes (2.2 × 2.2 mm each) connected to 12 rectangular reservoir electrodes (16.4 × 6.7 mm or 16.4 × 6.4 mm each). After patterning, substrates were coated with Parylene-C (7 μm) by evaporating 15 g of dimer in a vapor deposition instrument (Specialty Coating Systems). Substrates were then coated either with Teflon-AF (300–350 nm) or FPEG-FA (350–400 nm). Teflon-AF was spin-coated (1 wt/vol% in Fluorinert FC-40, 1500 rpm, 30 s) and then postbaked on a hot-plate (160 °C, 10 min). FPEG-FA was dip-coated in the respective copolymer solutions (1 wt/vol% in trifluorotoluene) for 3 minutes, after which substrates were removed, cured overnight at room temperature, and then annealed at 100°C for 6 h in an oven. Unpatterned top plates were formed by coating indium tin oxide (ITO)-coated glass substrates (Delta Technologies, Stillwater, MN) with Teflon-AF as above. Devices were assembled with top (coated with Teflon-AF) and bottom (coated with Teflon-AF or FPEG-FA) plates separated by a spacer formed from 2 pieces of double-sided tape (total thickness 140 μm). Unit droplets (i.e., those covering a single actuation electrode) in these devices were ≈4 μL for device one, ≈10 μL for device two, and ≈1.6 μL for device three. To actuate droplets, sine-wave driving potentials (180 V_{rms} for mobile droplets on device one, 110 V_{rms} for stationary droplets on device two, and 110 V_{rms} for mobile droplets on device three, all at 10 kHz) were generated by amplifying the output of a function generator (Agilent Technologies, Santa Clara), and were applied to sequential electrodes on the bottom plate relative to the electrode on the top plate. For devices one and two, potentials were applied to the electrodes manually; for device three, potentials were applied using an automated droplet control system described in detail elsewhere.[42]

DMF Device Longevity Analysis: DMF device longevity was evaluated using device one with methods described previously.[27] Briefly, RPMI 1640 cell culture medium was supplemented with 10% fetal bovine serum (FBS) (Life Technologies/Invitrogen Canada, Burlington, ON) and one of four Pluronic additives (w/v%): F68 (0.05), F88 (0.06), P105 (0.02), L92 (0.02). At least 3 droplets of each solution were evaluated on at least 2 different devices. Device failure was defined as any case in which a droplet required more than 15 seconds to complete a movement step from one electrode to the next, and the number of steps and the time until device failure were recorded for each condition.

AFM and XPS Analysis: AFM and XPS measurements were used to characterize DMF device-two bottom plates in either passive or activated state. Passive substrates were used without special preparation. Activated substrates were prepared by assembling a top and bottom plate and potentiating a stationary unit droplet of DI water for 10 min, supplementing with additional water when needed to compensate for evaporation. After activating, the devices were disassembled, the water was wicked away with a KimWipe, and the activated portion of the substrate was evaluated within 5–10 min (or in some cases, after one or several hours). A Dimension 5000 atomic force microscope (AFM) (Digital Instruments, Santa Barbara) was operated in tapping mode to obtain topographic and phase images using NCH rectangular shaped silicon probes (Nanoworld, Switzerland) with resonance frequencies in the range 280–320 kHz and a spring constant of 40 N/m. Force-distance curve measurements and indentation curves were collected using an MFP-3D Molecular Force Probe AFM (Asylum Research, Santa Barbara) and MLCT V-shaped silicon nitride cantilevers (Bruker, Santa Barbara), respectively. The cantilevers had a nominal spring constant of 0.05 N/m, and were calibrated before each experiment by the thermal noise method.[61] The resulting curves were analyzed with custom analysis software (Igor Pro, Wavemetrics). XPS spectra were acquired at Surface Interface Ontario using a Thermo Scientific Theta Probe (East Grinstead, UK) utilizing monochromatic Al K-alpha X-rays for excitation. The emission angle was 50 degrees (relative to surface normal), which probes a sampling depth of 8–10 nm. Regional spectra (C1s) were acquired at high energy resolution and processed using Avantage software (Thermo Scientific). A Shirley background function was used to approximate the experimental backgrounds. Surface elemental compositions were calculated from background-subtracted peak areas derived from transmission function-corrected regional spectra. Scofield Al K-alpha sensitivity factors were used to calculate the relative atomic percentages. Spectra were collected from three separate regions on two different devices for each condition.

Contact Angle Studies: Contact angles were measured with a Kruss DSA100 (Hamburg, Germany) goniometer at room temperature, using the sessile drop fitting method (Drop Shape Analysis System) for 5 μL droplets of water and hexadecane. The substrates were DMF device-two

bottom plates (with no top plate). Prior to analysis, a top/bottom plate device was assembled and a unit droplet of DI water (stationary, positioned over one electrode) was potentiated for 0, 2, 4, 6, 8, or 10 min. During this activation process, when necessary, additional DI water was added to compensate for evaporation. After potentiation, the water was wicked away, the device was disassembled, and a (fresh) interrogating droplet was positioned above the electrode surface that had been potentiated. Contact angle measurements were recorded from 3 devices (6 readings each) for both of the interrogating liquids.

Supporting Information

Supporting Information is available from the Wiley Online Library or from the author.

Acknowledgements

The authors thank the Ontario Institute for Cancer Research (OICR) and the Natural Sciences and Engineering Research Council of Canada (NSERC) for funding. GW and ARW thank the Canada Research Chair (CRC) program for CRCs. The authors thank Professor Eugenia Kumacheva (Department of Chemistry, University of Toronto) for use of the contact angle goniometer and Dr. Sam Au (Univ. Toronto), Dr. Irena Barbulovic-Nad (Univ. Toronto), Prof. Robin Ras (Aalto Univ.), and Prof. Shashi Murthy (Northeastern Univ.) for helpful discussions.

Received: July 4, 2014
Revised: October 17, 2014
Published online: November 20, 2014

[1] O. Flogel, J. D. Codee, D. Seebach, P. H. Seeberger, *Angew. Chem.* **2006**, *45*, 7000.
[2] Y. Kikutani, T. Horiuchi, K. Uchiyama, H. Hisamoto, M. Tokeshi, T. Kitamori, *Lab Chip* **2002**, *2*, 188.
[3] A. Nagaki, H. Kim, H. Usutani, C. Matsuo, J. Yoshida, *Org. Biomol. Chem.* **2010**, *8*, 1212.
[4] A. Palmieri, S. V. Ley, K. Hammond, A. Polyzos, I. R. Baxendale, *Tetrahedron Lett.* **2009**, *50*, 3287.
[5] B. K. Yen, A. Gunther, M. A. Schmidt, K. F. Jensen, M. G. Bawendi, *Angew. Chem.* **2005**, *44*, 5447.
[6] J. C. Pastre, D. L. Browne, S. V. Ley, *Chem. Soc. Rev.* **2013**, *42*, 8849.
[7] K. Choi, A. H. Ng, R. Fobel, A. R. Wheeler, *Annu. Rev. Anal. Chem.* **2012**, *5*, 413.
[8] M. J. Jebrail, A. H. Ng, V. Rai, R. Hili, A. K. Yudin, A. R. Wheeler, *Angew. Chem.* **2010**, *49*, 8625.
[9] M. J. Jebrail, A. R. Wheeler, *Anal. Chem.* **2009**, *81*, 330.
[10] P. Y. Keng, S. Chen, H. Ding, S. Sadeghi, G. J. Shah, A. Dooraghi, M. E. Phelps, N. Satyamurthy, A. F. Chatziioannou, C.-J. C. Kim, R. M. van Dam, *Proc. Natl. Acad. Sci. USA* **2012**, *109*, 690.
[11] D. Witters, N. Vergauwe, R. Ameloot, S. Vermeir, D. De Vos, R. Puers, B. Sels, J. Lammertyn, *Adv. Mater.* **2012**, *24*, 1316.
[12] M. Jebrail, N. Assem, J. Mudrik, M. Dryden, K. Lin, A. Yudin, A. Wheeler, *J. Flow Chem.* **2012**, *2*, 103.
[13] I. Barbulovic-Nad, S. H. Au, A. R. Wheeler, *Lab Chip* **2010**, *10*, 1536.
[14] D. Bogojevic, M. D. Chamberlain, I. Barbulovic-Nad, A. R. Wheeler, *Lab Chip* **2012**, *12*, 627.
[15] S. Srigunapalan, I. A. Eydelnant, C. A. Simmons, A. R. Wheeler, *Lab Chip* **2012**, *12*, 369.
[16] I. A. Eydelnant, B. Betty Li, A. R. Wheeler, *Nat. Commun.* **2014**, *5*, 3355.
[17] D. Witters, N. Vergauwe, S. Vermeir, F. Ceyssens, S. Liekens, R. Puers, J. Lammertyn, *Lab Chip* **2011**, *11*, 2790.
[18] S.-K. Fan, P.-W. Huang, T.-T. Wang, Y.-H. Peng, *Lab Chip* **2008**, *8*, 1325.
[19] P. Kim, H. E. Jeong, A. Khademhosseini, K. Y. Suh, *Lab Chip* **2006**, *6*, 1432.
[20] S. Lee, J. Vörös, *Langmuir* **2005**, *21*, 11957.
[21] M. Ebara, J. M. Hoffman, P. S. Stayton, A. S. Hoffman, *Radiat. Phys. Chem.* **2007**, *76*, 1409.
[22] H. Bi, W. Zhong, S. Meng, J. Kong, P. Yang, B. Liu, *Anal. Chem.* **2006**, *78*, 3399.
[23] V. Srinivasan, V. K. Pamula, R. B. Fair, *Lab Chip* **2004**, *4*, 310.
[24] A. P. Aijian, D. Chatterjee, R. L. Garrell, *Lab Chip* **2012**, *12*, 2552.
[25] J.-Y. Yoon, R. L. Garrell, *Anal. Chem.* **2003**, *75*, 5097.
[26] H. Yang, V. N. Luk, M. Abelgawad, I. Barbulovic-Nad, A. R. Wheeler, *Anal. Chem.* **2008**, *81*, 1061.
[27] S. H. Au, P. Kumar, A. R. Wheeler, *Langmuir* **2011**, *27*, 8586.
[28] V. N. Luk, G. C. H. Mo, A. R. Wheeler, *Langmuir* **2008**, *24*, 6382.
[29] G. Perry, V. Thomy, M. R. Das, Y. Coffinier, R. Boukherroub, *Lab Chip* **2012**, *12*, 1601.
[30] Y. Cho, H. S. Sundaram, J. A. Finlay, M. D. Dimitriou, M. E. Callow, J. A. Callow, E. J. Kramer, C. K. Ober, *Biomacromolecules* **2012**, *13*, 1864.
[31] S. Krishnan, R. Ayothi, A. Hexemer, J. A. Finlay, K. E. Sohn, R. Perry, C. K. Ober, E. J. Kramer, M. E. Callow, J. A. Callow, D. A. Fischer, *Langmuir* **2006**, *22*, 5075.
[32] S. Krishnan, N. Wang, C. K. Ober, J. A. Finlay, M. E. Callow, J. A. Callow, A. Hexemer, K. E. Sohn, E. J. Kramer, D. A. Fischer, *Biomacromolecules* **2006**, *7*, 1449.
[33] Z. Zhao, H. Ni, Z. Han, T. Jiang, Y. Xu, X. Lu, P. Ye, *ACS Appl. Mater. Interfaces* **2013**, *5*, 7808.
[34] D. P. Papageorgiou, E. P. Koumoulos, C. A. Charitidis, A. G. Boudouvis, A. G. Papathanasiou, *J. Adhes. Sci. Technol.* **2012**, *26*, 2001.
[35] D. P. Papageorgiou, A. Tserepi, A. G. Boudouvis, A. G. Papathanasiou, *J. Colloid Interface Sci.* **2012**, *368*, 592.
[36] A. Schultz, S. Chevalliot, S. Kuiper, J. Heikenfeld, *Thin Solid Films* **2013**, *534*, 348.
[37] R. F. Brady, I. L. Singer, *Biofouling* **2000**, *15*, 73.
[38] M. K. Chaudhury, J. A. Finlay, J. Y. Chung, M. E. Callow, J. A. Callow, *Biofouling* **2005**, *21*, 41.
[39] J. Y. Chung, M. K. Chaudhury, *J. Adhesion* **2005**, *81*, 1119.
[40] S. Krishnan, C. J. Weinman, C. K. Ober, *J. Mater. Chem.* **2008**, *18*, 3405.
[41] J. A. Callow, M. E. Callow, *Nat. Commun.* **2011**, *2*, 244.
[42] R. Fobel, C. Fobel, A. R. Wheeler, *Appl. Phys. Lett.* **2013**, *102*, 193513.
[43] M. A. C. Stuart, W. T. S. Huck, J. Genzer, M. Muller, C. Ober, M. Stamm, G. B. Sukhorukov, I. Szleifer, V. V. Tsukruk, M. Urban, F. Winnik, S. Zauscher, I. Luzinov, S. Minko, *Nat. Mater.* **2010**, *9*, 101.
[44] E. Martinelli, S. Agostini, G. Galli, E. Chiellini, A. Glisenti, M. E. Pettitt, M. E. Callow, J. A. Callow, K. Graf, F. W. Bartels, *Langmuir* **2008**, *24*, 13138.
[45] S.-J. Ding, P.-F. Wang, X.-G. Wan, D. W. Zhang, J.-T. Wang, W. W. Lee, *Mater. Sci. Eng. B* **2001**, *83*, 130.
[46] J. Lahann, S. Mitragotri, T.-N. Tran, H. Kaido, J. Sundaram, I. S. Choi, S. Hoffer, G. A. Somorjai, R. Langer, *Science* **2003**, *299*, 371.
[47] W.-S. Yeo, M. N. Yousaf, M. Mrksich, *J. Am. Chem. Soc.* **2003**, *125*, 14994.
[48] P. Shivapooja, Q. Wang, B. Orihuela, D. Rittschof, G. P. López, X. Zhao, *Adv. Mater.* **2013**, *25*, 1430.
[49] M. Abdelgawad, A. R. Wheeler, *Adv. Mater.* **2007**, *19*, 133.
[50] V. Pillay, T.-S. Tsai, Y. E. Choonara, L. C. du Toit, P. Kumar, G. Modi, D. Naidoo, L. K. Tomar, C. Tyagi, V. M. K. Ndesendo, *J. Biomed. Mater. Res. A* **2014**, *102*, 2039.
[51] J. Hu, S. Liu, *Macromolecules* **2010**, *43*, 8315.

[52] J. Shi, A. R. Votruba, O. C. Farokhzad, R. Langer, *Nano Lett.* **2010**, *10*, 3223.
[53] J. Lee, H. Moon, J. Fowler, T. Schoellhammer, C.-J. Kim, *Sens. Actuators A* **2002**, *95*, 259.
[54] H. Moon, S. K. Cho, R. L. Garrell, C.-J. C. Kim, *J. Appl. Phys.* **2002**, *92*, 4080.
[55] J. A. Howarter, J. P. Youngblood, *Adv. Mater.* **2007**, *19*, 3838.
[56] T. Chen, R. Ferris, J. Zhang, R. Ducker, S. Zauscher, *Prog. Polym. Sci.* **2010**, *35*, 94.
[57] H. Kuroki, I. Tokarev, S. Minko, *Annu. Rev. Mater. Res.* **2012**, *42*, 343.
[58] I. T. S. Li, G. C. Walker, *J. Am. Chem. Soc.* **2010**, *132*, 6530.
[59] I. T. S. Li, G. C. Walker, *Acc. Chem. Res.* **2012**, *45*, 2011.
[60] K. Choi, A. H. Ng, R. Fobel, D. A. Chang-Yen, L. E. Yarnell, E. L. Pearson, C. M. Oleksak, A. T. Fischer, R. P. Luoma, J. M. Robinson, J. Audet, A. R. Wheeler, *Anal. Chem.* **2013**, *85*, 9638.
[61] J. L. Hutter, J. Bechhoefer, *Rev. Sci. Instrum.* **1993**, *64*, 1868.